

Electric field effects on force curves for oxidized silicon tips and ice surfaces in a controlled environment

C. R. Slaughterbeck, E. W. Kukes, B. Pittenger, D. J. Cook, P. C. Williams, V. L. Eden, and S. C. Fain, Jr.^{a)}

Department of Physics, University of Washington, Seattle, Washington 98195-1560

(Received 4 October 1995; accepted 4 December 1995)

A scanning force microscope and environmental chamber are described for use in studying the surface properties of ice that is grown from vapor. This microscope uses a modulated optical deflection scheme to minimize low frequency noise, and a thermal feedback system which can stabilize the ice temperature to within 0.4 mK. The ice crystal can be examined in its own vapor plus other controlled gaseous environments. Initial results show that, in the range of -8 to -10 °C and negative tip voltages, necks form between the oxidized silicon tip and the ice sample after contact with the surface. © 1996 American Vacuum Society.

I. INTRODUCTION

The study of ice interfaces has a long history, starting with a conflict between Faraday¹ and Thomson² in 1859 about the way that ice particles adhere to one another. Since ice is so plentiful on the earth, it has continued to be an often studied substance, in part because of the many environmental effects in which ice plays a role.³

Interfaces between ice and its vapor or other materials have been investigated by various techniques, including x-ray scattering,⁴ nuclear magnetic resonance (NMR),⁵ motion of a weighted solid wire through ice,⁶ ellipsometry,^{7,8} interference microscopy,⁷ frost heave dynamics,⁹ and scanning force microscopy (SFM).¹⁰ Some of these investigations reveal that a premelted layer exists at ice interfaces at temperatures below the melting point. The thickness and dynamic properties of this quasi-liquid layer (QLL) are under dispute. Since water is an ionizable, polar molecule, an applied electric field could change the properties of this QLL.¹¹ It is known that electric fields do change the kinetics of ice growth,¹² diffusion of Pt,¹³ and contact angles of ionic surfactant and electrolyte solution.¹⁴

SFM¹⁵ has been used to study the surface properties of liquid layers on top of solid surfaces¹⁶ as well as the electrostatic properties of surfaces.¹⁷ We have built a SFM that is used for measuring electrostatic effects on the mechanical properties of the surface of ice at temperatures from -20 ° to 0 °C.

II. MECHANICAL APPARATUS

The overall design of the instrument can be seen in Figure 1. The SFM uses optical deflection to measure the bending of the silicon cantilevers.¹⁸ Polarized light is emitted from a diode laser (wavelength 670 nm). The laser is oriented in such a manner that the light is completely reflected from the polarizing beam splitter down the principal axis of the instrument. After leaving the beam splitter cube, the light passes through a quarter-wave plate on the way to the cantilever.

The light passes through the quarter-wave plate twice, once going down the piezo tube and once coming back after reflecting off of the cantilever. Thus in essence, it will act like a half-wave plate and rotate the polarization of the light 90°, allowing it to pass straight through the beam splitter to the photodiode detector. One advantage of this design is that it is fairly symmetric and thus minimizes thermal drift in cantilever-sample separation. The detector is split into quadrants for simultaneous detection of normal and frictional forces.¹⁹

The microscope head and environmental chamber are depicted in Figure 2. The silicon chip, from which the silicon cantilever extends, is attached to steel shim stock by cement and/or conductive silver print.²⁰ The steel is held onto the microscope body with an electrically conducting magnet. Electrical connections to the tip are made by painting a line of silver print from the magnet over the vacuum seal to a connection outside of the chamber.

The sample block is made of gold plated copper. A thermoelectric cooler²¹ is soldered onto the front of the sample block with InSn solder. The edges of the cooler are sealed against moisture by a silicone sealant.²² Heat expelled from the coolers is transferred via the copper block to the environment away from the cold surface. The temperature is measured with a small bead thermistor²³ that is attached to the cold side of the thermoelectric cooler with thermal grease and tacked down with cement. The cold side of the thermoelectric cooler is also covered with InSn solder that has been rough polished. An electrical connection is maintained to the solder on which the ice is grown by a line of conductive silver print.²⁰ Wires run along the sample block for the thermoelectric cooler and the thermistor. Smaller wires are glued into the back of the small glass vacuum chamber and attached to the sample block, thermoelectric cooler wires, and thermistor wires at the back of the sample block.

The sample block rests on two tungsten carbide rails that are attached to the outer piezo tube. For a coarse approach or retraction, a sawtooth wave voltage can be put across the walls of the piezo tube, causing it to walk the sample block

^{a)}Electronic mail: fain@phys.washington.edu

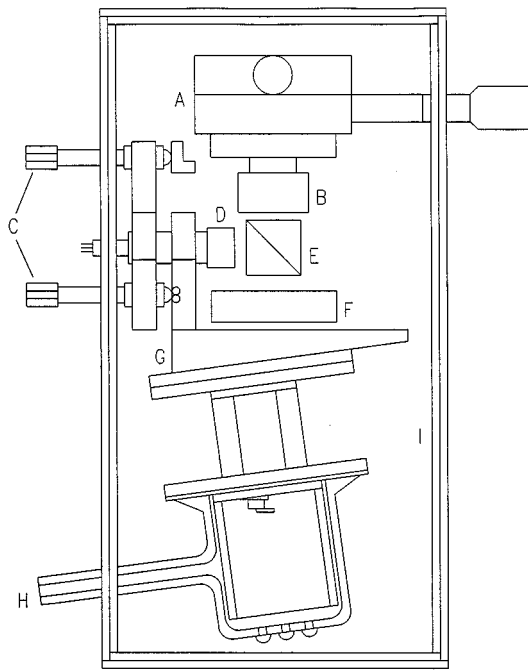


FIG. 1. Scanning force microscope. A: X-Y micropositioner for photodiode adjustment. B: quadrant photodiode and housing. C: X-Y laser diode aiming adjustment (80 turns per inch screws). D: diode laser and focusing lens. E: polarizing beam splitter cube. F: quarter-wave plate. G: angle bracket for piezo mounting flanges. H: glass vacuum chamber. I: copper cold shield.

in towards the cantilever and tip or out away from them, depending on the polarity of the voltage.²⁴

The cantilever and tip are mounted on the inner piezo tube which is mounted concentrically with the outer piezo tube. The concentric mounting scheme helps to minimize thermal drifts while providing mechanical stability. The piezo tubes are sealed together at one end with silicone sealant.²² This silicone is necessary to provide a vacuum seal for the environmental chamber and keep the water vapor away from the high voltage piezo leads while simultaneously allowing the piezo tubes some degree of flexibility.

The end of the inner tube is sealed with a glass microscope cover slip which has been glued to the tip holder and inner piezo tube. The glass provides an excellent vacuum seal while still allowing the laser beam used for optical deflection to pass from the optical part of the microscope into the sample chamber.

The sample chamber itself is made of glass that seals onto a glass ring that is glued onto the end of the outer piezo tube. The seal is made with a thin silicone gasket and vacuum grease. The chamber is held tight against the gasket by the differential pressure between atmosphere and vacuum. The principal advantage of this type of seal is the ease of taking it on and off for tip exchange and alignment. The chamber itself is very small—about 20 cm³, and a large part of this volume is occupied by the sample block itself. This design minimizes dead volume in the chamber and helps keep crystal thickness fluctuations small since the size of the fluctuations is proportional to the ratio of the chamber dead volume to ice surface area.

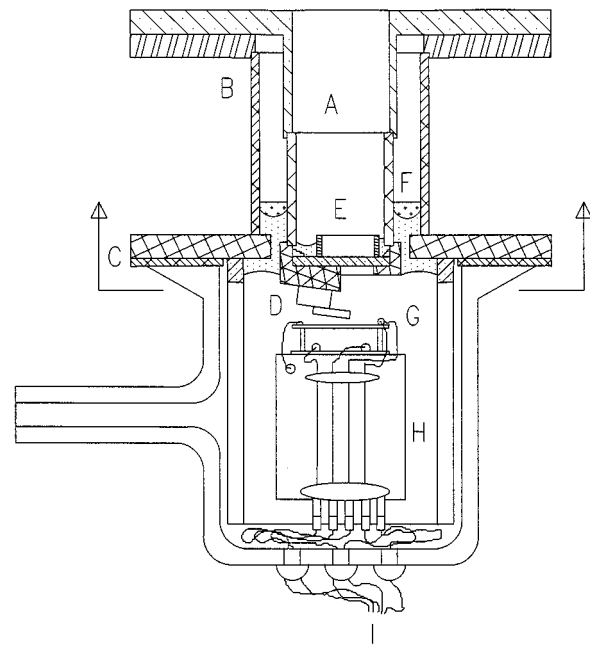


FIG. 2. SFM head and environmental chamber. A: inner piezo tube and mounting flange. B: outer piezo tube and mounting flange. C: glass surface for mounting vacuum chamber. D: magnetic tip holder and mounting bracket. E: glass flat which is glued to inner piezo tube. F: silicone sealant between piezo tubes. G: thermoelectric cooler for ice growth and thermistor. H: gold coated copper sample block. Electrical leads to the thermoelectric cooler and thermistor (G) are glued to the side of the block. I: wire vacuum feedthroughs are sealed with cement.

The vacuum line leading from the chamber is attached to a Pirani pressure gauge, a capacitance manometer pressure gauge for use at $P < 10$ Torr, as well as a line that can be connected to a source of gas (dry N₂ or CO₂) or water. The water is triply distilled, de-ionized to 18 MΩ cm, and then degassed by repeatedly freezing it and pumping off the gas that was expelled from the ice. Ice is grown on the sample by cooling the sample holder to less than -15 °C and then dosing the water vapor into the evacuated sample chamber in small increments. The ice grown in this manner is probably polycrystalline and is approximately 100 μm thick. The experiments described here were performed under pure water vapor. In other experiments we later added N₂ or CO₂ gas to slow down the surface-vapor dynamics. Note that the presence of different atmospheres may also affect the physical properties of the QLL.

The entire SFM is mounted in a copper cold shield which is cooled by three thermoelectric coolers,²¹ capable of cooling the cold shield about 20 °C below ambient temperature. The cold shield sits on top of an aluminum block which is hung from the ceiling with rubber vacuum tubing to provide vibration isolation. The aluminum block is partially immersed in an automotive antifreeze and water bath which can be periodically cooled with liquid nitrogen. This bath, plus the thermoelectric coolers on the cold shield and the thermoelectric cooler on the sample block, allow us to investigate the behavior of ice at temperatures as low as -25 °C.

Because we are concerned about heating the tip with the

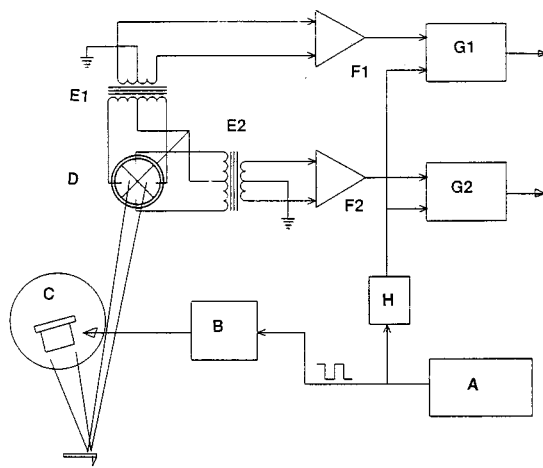


FIG. 3. Modulated laser deflection scheme. A: 66 kHz oscillator. B: laser driver and protection. C: laser diode. D: quadrant photodiode. E1 and E2: differentiating transformers. F1 and F2: high gain single stage transconductance amplifiers. G1 and G2: phase sensitive detectors and filters. H: 90° phase shifter.

laser light and unintentionally melting the ice, we have measured the energy reaching our cantilever from the laser as a function of laser current with a calibrated photodiode. We typically operate in the range of 1–5 μW of power incident upon the cantilever. Calculations for our cantilevers similar to those made by Eastman and Zhu²⁵ indicate that laser heating effects will be very small for such low laser powers.

While the temperature of the tip is not affected by the low laser power, it is influenced by the temperature of the microscope. In order to perform this experiment, the ice substrate must be the coldest location in the chamber. If the substrate is not the coldest location in the chamber, the ice will nucleate at the colder location instead of on the substrate. If the temperature of some part of the chamber becomes colder than the substrate during the course of the experiment, the ice will move to that colder location by vapor transport fairly quickly. In particular, it is important to note that this experiment cannot be performed under isothermal conditions, meaning that the tip must be slightly warmer than the ice.

The tip temperature is difficult to measure because of the small size of the cantilever. The tip temperature is primarily influenced by the temperature of the microscope body to which it is attached and the temperature of the ice which is only a few microns away. As noted above, the microscope body must be warmer than the ice. We have varied the temperature of the microscope body from 1 to 7 °C warmer than the ice without noticeably affecting the results of our experiments. We conclude, therefore, that the tip temperature is most strongly influenced by the temperature of the ice.

III. ELECTRONICS

As mentioned above, we use the optical deflection method to determine the deflection of our cantilever above the ice sample. Conventional dc detection schemes can be sensitive to 60 Hz noise, which is unfortunately near the range of

interest in our measurements. We have therefore elected to use ac techniques to measure the deflection of the lever, depicted in Figure 3. The diode laser is modulated at 66 kHz. The current produced by this signal in the photodiode is amplified in a resonant transformer coupled preamplifier. The resonant transformer coupled preamplifier provides several advantages over dc schemes: (1) Common mode gain is killed in the first stage, since the transformers provide gain for only the difference between the left and right (or up and down) quadrant inputs of the photodiode. (The second deflection output has so far been used only for adjusting the photodiode position.) (2) There is more gain in the first stage, providing a higher signal to noise ratio. (3) There is much improved immunity to $1/f$ noise and 60 Hz line noise.

After further amplification in high gain single stage transconductance amplifiers, the signal is demodulated by a phase sensitive detector and filter before routing to the conventional scanning tunneling microscopy control electronics,²⁶ which is controlled by a 386 personal computer. We have modified the source code of the software to allow for acquisition and analysis of complete bidirectional force–distance (FZ) curves.

The Z motion of each piezo is calibrated by measuring the interference produced during a FZ curve by light reflected from the cantilever and light diffusely scattered by the sample. We found that the piezo response was nonlinear and that both the linear and quadratic coefficients of expansion as a function of applied voltage varied with temperature. The data are corrected for these effects during analysis.

The optical gain of the microscope is defined as the ratio of δx , the distance that the spot moves at the detector, to δz , the distance the tip is deflected. A simple geometrical analysis gives the optical gain as

$$\frac{\delta x}{\delta z} = \frac{AL}{l}, \quad (1)$$

where L is the distance from the cantilever to the photodiode, l is the length of the cantilever, and A is a geometrical constant that depends on the way that the cantilever bends. If the cantilever is modeled as a rigid beam that pivots about the point where it is connected to the silicon chip, then $A=2$. If the cantilever is modeled as a flexible beam with constant cross section and the force acts at the end of the cantilever,²⁷ then $A=3$. In our experiments, the cantilever is neither perfectly rigid, nor does it have constant cross section, thus we calibrate A . The calibration is performed by taking a FZ curve on a glass microscope cover slip. Since the glass slide does not yield under the pressure of the tip, we can calculate A by measuring the optical gain directly. For the 180- μm -long cantilevers used here, we find $A=2.1$.

The thermistor attached to the thermoelectric cooler was calibrated by measuring the thermistor resistance and the temperature when the thermistor was immersed in a large, insulated bath of alcohol. The accuracy of the temperature measurements is estimated as ± 0.2 °C. The temperature is maintained at a constant value by a feedback circuit connected to the thermoelectric cooler.

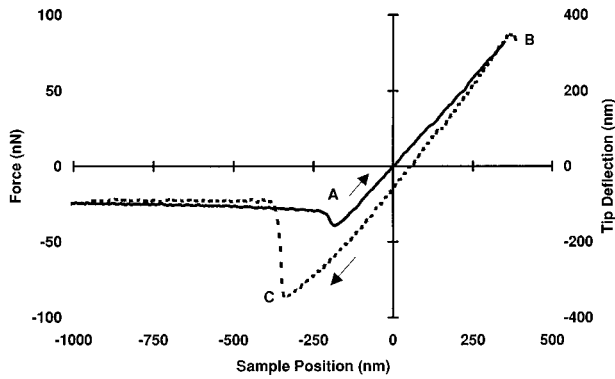


FIG. 4. *FZ* curve taken on ice at -8°C with $+10\text{ V}$ bias on the cantilever and tip. Acquisition time was 34 ms. The solid curve is approach to surface, and the dashed curve is retraction from surface. The force zero is set at zero bias with the cantilever at least $1\ \mu\text{m}$ away from the surface. The position zero is set to be zero for zero force acting on the tip during the approach.

When doing experiments on ice, it is extremely important to maintain temperature stability. The steep slope of the ice/vapor coexistence line ($dP/dT=0.375\text{ Torr}/^{\circ}\text{C}$ at the melting point) means that small temperature fluctuations lead to large fluctuations in the equilibrium vapor pressure, which cause the surface to grow or sublimate away quickly. The stability of the feedback circuit in our system limits fluctuations to $<0.4\text{ mK}$.

FZ curves in our system are performed by moving the cantilever in toward the sample a distance of about $1.5\ \mu\text{m}$ and then pulling it back about $1.5\ \mu\text{m}$. The speed is approximately constant during approach and retraction. The complete curve is taken in as little as 34 ms, or as long as 8 s. In addition, we can shorten the distance that the cantilever moves in and out, although this made the *FZ* curves on ice difficult to interpret because the tip was typically not free of surface forces unless the full $1.5\ \mu\text{m}$ range was used. The electronics setup in our system imposes one further limitation; it takes 175 ms to transfer the data taken in a *FZ* curve back to the computer before we can take another curve. Thus, we cannot investigate changes from one *FZ* curve to the next on a faster time scale.

Since we are using a conductive silicon cantilever and tip, we can put a bias on the tip with respect to the InSn below the ice. The software allows us to vary the potential of the tip from -10 to $+10\text{ V}$ while holding the cantilever base at a fixed position above the ice surface. The result is a measurement of the force on the tip versus applied voltage. Typical curves were quadratic in voltage with a minimum attractive force near 0 V .

IV. RESULTS

Figure 4 shows a *FZ* curve taken in 34 ms for an oxidized silicon tip interacting with an ice sample in pure water vapor at -8°C with $+10\text{ V}$ of bias on the tip. Notice that the force acting on the cantilever at a distance of $1\ \mu\text{m}$ is already attractive (the zero of force was set for zero applied voltage). Electrostatic forces between the positively biased cantilever and the ice and the grounded InSn solder on which the ice is

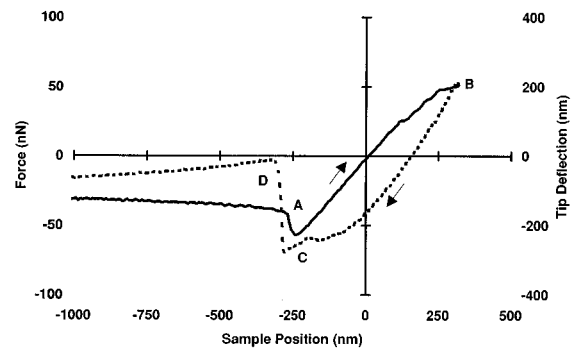


FIG. 5. *FZ* curve taken on ice at -8°C with -10 V bias on the tip and cantilever. Other parameters are the same as in Figure 4.

grown are attractive, with little variation over the first $0.7\ \mu\text{m}$ motion. The total force becomes more attractive as the tip approaches the sample within a distance comparable to the tip radius. The force gradient becomes stronger than the cantilever spring constant and the cantilever snaps into contact with the ice surface²⁷ at point A. As the cantilever base continues to move toward the surface, the tip contacts the ice, with a maximum repulsive force of about 80 nN at point B. As the tip deflection is approximately equal to the cantilever displacement, the tip does not appreciably indent the ice. The cantilever base then is withdrawn from the ice but the tip stays on the ice. Note that the ice surface has slightly receded locally due to the presence of the cantilever and tip, as the tip does not exactly retrace the approach curve. Since the tip adheres to the ice, the tip stays on the surface of the ice past the point where it jumped to contact. Finally, when the force reaches -80 nN at point C, the tip snaps off the surface of the ice²⁷ and returns to approximately the same value it had on the approach.

The process of taking *FZ* curves on the sample is repeated approximately once per second in order to watch how the *FZ* curves change over time. Typically, we see the ice sample recede from the tip with time. The rate of this recession depends on many things, including whether the tip is touching the sample between measurements, the proximity of the cantilever to the sample if they are not actually touching, and the presence of gases in addition to the water vapor above the sample. The speed of recession varies from a few seconds to tens of minutes for the surface to move outside the $1.5\ \mu\text{m}$ range of our piezo.

Figure 5 is a typical curve taken in 34 ms at -8°C with -10 V of bias on the tip. Similar to the curve in Figure 4, the force is already attractive a distance of $1\ \mu\text{m}$ away from the surface due to attractive electrostatic forces between the cantilever and ice. Once again, the tip snaps towards the surface at point A due to the strong force gradient. The tip touches the ice surface and digs in slightly as the force gradually increases up to about 50 nN at point B. Note that the retraction curve lies to the right of the approach curve by as much as $0.15\ \mu\text{m}$. This shows that the local surface of the ice has moved away from the cantilever and tip more than in Figure 4. At point C, there is a significant difference between Fig-

ures 4 and 5. With +10 V bias applied to the tip in Figure 4, the tip stayed on the surface of the ice until it snapped off and returned to the same force it had during approach. With -10 V applied to the tip in Figure 5, the tip feels a region of approximately constant force for 200 nm before snapping free of the surface. The small wiggles at $-0.2 \mu\text{m}$ are not typical, but a region of approximately constant force has been observed reproducibly.

The observation of a region of constant force while the cantilever and tip are being pulled back indicates that the tip feels an attractive force that does not change much with distance from the equilibrium surface position. Then it suddenly snaps free of the surface. This phenomenon is what one would expect if a neck were being formed by mass flow between the tip and the ice. The neck breaks when the mass flow is insufficient to maintain a complete connection.

When the tip snaps off the surface to point D, the cantilever does not return to the same deflection it had on approach; it is less attractive. This is due to charge transferred from the ice surface to the cantilever or tip. The charge decays away in less than 1 s since the next *FZ* curve follows the approach of that shown in Figure 5. The amount of charge transferred and its decay rate depend on the cantilever and the ice sample. However it is always larger at -10 than +10 V.

The data in Figures 4 and 5 were taken with the same tip a few minutes apart and the principal features of the curves have been repeated on other days with different cantilevers and ice samples. At low temperatures ($< -10 \text{ }^\circ\text{C}$), we do not observe necking, nor do we observe this type of behavior for every cantilever and ice sample. We have observed the necking phenomenon at biases between -10 and 0 V in the temperature range -10 to $-8 \text{ }^\circ\text{C}$. At higher temperatures, necking sometimes occurs at positive tip biases as well.

There have been two different necking phenomena observed by scanning probe microscopes. Mate, Lorenz, and Novotny¹⁶ have observed liquid necks which form when they retract a probe tip from a silicon surface covered with polymeric liquid films. In that case, the liquid neck formed when the tip was wetted by the polymer films and the neck lasted up to 275 nm before the tip snapped away from the liquid. Kuipers, Frenken, and Hoogeman have observed solid necks which formed between their scanning tunneling microscope tip and the Pb(110) (Ref. 28) and Pb(111) (Ref. 29) surfaces at temperatures well below the onset of surface melting on Pb(110). In their experiment, they found that the length of the neck that formed was a function of both tip retraction velocity and temperature. They attributed the necks to surface diffusion of Pb atoms. In both the polymer film study of Mate, Lorenz, and Novotny and the lead study of Kuipers, Frenken, and Hoogeman, the necks were of comparable size to those that we observe in Figure 5.

In the case of ice, the surface at -8 to $-10 \text{ }^\circ\text{C}$ may be covered by a thin QLL. The thickness of any QLL should be quite dependent on environmental conditions, which may explain the large range of results for its thickness from other experiments.^{4,6-9} In addition, results for flat ice-vapor inter-

faces are not necessarily relevant to a 20-nm-radius tip that can produce curvature and interfacial premelting effects or capillary condensation. Due to the small thickness inferred for interfacial premelting at $-10 \text{ }^\circ\text{C}$,^{7,9,11} it seems unlikely that a quasi-liquid neck forms between our tip and the ice surface.

The surface diffusion coefficient of ice deduced from NMR measurements⁵ is $10^{-13} \text{ cm}^2/\text{s}$, two orders of magnitude larger than the bulk diffusion coefficient. Since ice is so mobile on the surface, it is also possible that the molecules can diffuse across the surface of the ice and build up a solid tip as observed in the Pb experiments of Kuipers, Frenken, and Hoogeman. In the case of ice, vapor transport from the flat ice surface to the neck must also be considered.³⁰ We are continuing our investigations of the necks and the roles that temperature, tip velocity, tip bias, and environment at the ice surface play in their formation.

V. CONCLUSIONS

We have built a scanning force microscope designed to measure *FZ* curves on the surface of ice in its own vapor as well as other controlled atmospheres. Some *FZ* curves taken with this apparatus show necking behavior that may be due to solid necks as seen by Kuipers, Frenken, and Hoogeman on the Pb (110) and (111) surfaces.^{28,29}

The mechanism for the growth of the neck and its dependence on the polarity of the electric field remain unclear. One possibility is that the junction between the ice and the InSn solder creates a contact potential which provides an offset from zero voltage. We judge that this is unlikely, since such a contact potential would need to be in the neighborhood of 5 V, which seems rather high. We believe that it is more likely that ions at the surface of the ice explain our observations. The observation of charging as seen in Figure 5 indicates that there are mobile ions on the ice surface that move in response to the tip's electric field. If these mobile ions have positive charge, they will be attracted to the negatively charged tip. Such a charged surface region may induce the necks to form.

If the growth mechanism for the neck is surface or volume diffusion, one would expect that the length of the neck formed in these experiments would depend on retraction velocity as in the Pb experiments of Kuipers, Frenken, and Hoogeman.^{28,29} We have been unable to test this hypothesis in a pure water vapor environment since the surface moves away from the tip too quickly when the tip is in contact with the surface for us to significantly slow down the approach curve, and the electronics we use cannot take the data any faster.

ACKNOWLEDGMENTS

The authors wish to thank M. B. Baker, J. G. Dash, J. Frenken, D. Joswiak, D. Lamb, B. Mason, M. Mate, R. C. McAllister, V. Petrenko, and L. Wilen for their helpful discussions or assistance related to this work. This work was supported by National Science Foundation Grant No. DMR-

91-19701, with additional contributions by the University of Washington Graduate School Research Fund and McAllister Technical Services.

- ¹M. Faraday, *Philos. Mag.* **17**, 162 (1859).
- ²J. Thomson, *Proc. R. Soc. London Ser. A* **11**, 198 (1861).
- ³J. G. Dash, H. Fu, and J. S. Wettlaufer, *Rep. Prog. Phys.* **58**, 115 (1995).
- ⁴H. Dosch, A. Lied, and J. H. Bilgram, *Surf. Sci.* **327**, 145 (1995).
- ⁵Y. Mizuno and N. Hanafusa, *J. Phys. (Paris)* **48**, 511 (1987).
- ⁶R. R. Gilpin, *J. Coll. Interface Sci.* **77**, 435 (1980).
- ⁷D. Beaglehole and P. Wilson, *J. Phys. Chem.* **98**, 8096 (1994).
- ⁸M. Elbaum, S. G. Lipson, and J. G. Dash, *J. Cryst. Growth* **129**, 491 (1993).
- ⁹L. A. Wilen and J. G. Dash, *Phys. Rev. Lett.* **74**, 5076 (1995).
- ¹⁰O. Nickolayev and V. Petrenko, *Mater. Res. Soc. Symp. Proc.* **355**, 221 (1995).
- ¹¹L. Wilen, J. S. Wettlaufer, M. Elbaum, and M. Schick, *Phys. Rev. B* **52**, 12426 (1995).
- ¹²L. F. Evans, *J. Atmos. Sci.* **30**, 1657 (1973).
- ¹³G. L. Kellogg, *Appl. Surf. Sci.* **76-77**, 115 (1994).
- ¹⁴S. Wahal, C. Owiti, and A. Bose, *J. Adhesion Sci. Technol.* **7**, 519 (1993).
- ¹⁵G. Binnig, C. F. Quate, and Ch. Gerber, *Phys. Rev. Lett.* **56**, 930 (1986).
- ¹⁶C. M. Mate, M. R. Lorenz, and V. J. Novotny, *J. Chem. Phys.* **90**, 7550 (1989).
- ¹⁷B. D. Terris, J. E. Stern, D. Rugar, and H. J. Mamin, *Phys. Rev. Lett.* **63**, 876 (1989).
- ¹⁸We use Ultralevers from Park Scientific Instruments, 1171 Borregas Ave., Sunnyvale, CA 94089. The cantilever and tip are manufactured from heavily doped silicon and are covered with a thin layer of oxide. The force constant for the data shown is estimated to be 0.25 N/m. The radius of curvature for the tip used for Figs. 4 and 5 was determined by scanning electron microscopy to be less than 20 nm after the measurements shown here.
- ¹⁹G. Meyer and N. M. Amer, *Appl. Phys. Lett.* **57**, 2089 (1990); O. Marti, J. Colchero, and J. Mlynek, *Nanotechnology* **1**, 141 (1990).
- ²⁰The cement used is Torr Seal from Varian Vacuum Products, 121 Harwell Ave., Lexington, MA 02173. The silver print used is from GC Electronics Corp., Rockford, IL 61102.
- ²¹Melcor Electronic Products Corp., 1040 Spruce St., Trenton, NJ 08648.
- ²²Dow Corning Corp., Midland, MI 48686-0994.
- ²³Thermometrics, 808 US Highway 1, Edison, NJ 08817.
- ²⁴J. W. Lyding, S. Skala, J. S. Hubacek, R. Brockenbrough, and G. Gamme, *Rev. Sci. Instrum.* **59**, 1897 (1988).
- ²⁵T. Eastman and D.-M. Zhu, *J. Coll. Interface Sci.* **172**, 297 (1995).
- ²⁶McAllister Technical Services, W. 280 Prairie, Coeur d'Alene, ID 83814.
- ²⁷D. Sarid, *Scanning Force Microscopy* (Oxford University Press, Oxford, 1991).
- ²⁸L. Kuipers and J. W. M. Frenken, *Phys. Rev. Lett.* **70**, 3907 (1993).
- ²⁹L. Kuipers, M. S. Hoogeman, and J. W. M. Frenken, *Surf. Sci.* **340**, 231 (1995).
- ³⁰P. V. Hobbs and B. J. Mason, *Philos. Mag.* **9**, 181 (1964).